2025 IEEE World Haptics Conference (WHC)
Suwon Convention Center, Suwon, Korea
July 8 ~ 11, 2025

Investigating and Predicting Impacts of Thermal Feedback on Human Sensation and Emotion

Chungman Lim*
AI Graduate School
Gwangju Institute of Science and Technology
Gwangju, South Korea
chungman.lim@gm.gist.ac.kr

Su-Yeon Kang*
School of AI Convergence
Gwangju Institute of Science and Technology
Gwangju, South Korea
suyeon.kang@gm.gist.ac.kr

Donghyeon Kim
AI Graduate School
Gwangju Institute of Science and Technology
Gwangju, South Korea
hayate1212@gm.gist.ac.kr

Hasti Seifi
School of Computing and Augmented Intelligence
Arizona State University
Tempe, USA
hasti.seifi@asu.edu

Gunhyuk Park
School of AI Convergence
Gwangju Institute of Science and Technology
Gwangju, South Korea
maharaga@gist.ac.kr

***Abstract*—Recent advancements in thermal device technology present new possibilities for conveying sensations and emotions in diverse applications. Yet, systematic investigations into the design parameters of thermal feedback and their effects on elicited sensations and emotions remain underexplored. To address this gap, we created 36 thermal feedback patterns by systematically varying the amplitude of change, rate of change, and indoor temperature, and applied them across three body sites on the hand, forearm, and upper arm. We then collected perceived intensity, valence, and arousal ratings from 12 participants. The results revealed the efficacy of the thermal design parameters. For example, the amplitude of change served as the primary parameter influencing the intensity and arousal ratings across body sites, while it affected valence only when thermal feedback was applied to the forearm and upper arm. Using the collected data, we developed a neural network to predict the intensity sensation and emotion ratings elicited by thermal feedback. Our model outperformed three baseline machine learning models and demonstrated strong alignment with non-linear sensory and emotional responses. We present four guidelines for designing thermal feedback and discuss implications for future research and applications in haptic design.**

***Index Terms*—Thermal feedback, Sensation, Emotion, Prediction model, Neural network**

I. Introduction

Over the last decades, thermal feedback has been integrated into various applications and scenarios in human-computer interaction (HCI). By delivering sensory stimuli through controlled temperature changes, thermal feedback enables users to experience realistic and immersive interactions, applied in virtual reality (VR) [1]–[4], gaming [5], [6], medical simulation [7], and automotive user interfaces [8].

Past research has explored the relationship between thermal sensations (i.e., "cool/hot") and various aspects of cognition, such as social behaviors [9], interpersonal warmth [10], and metaphors [11]. Several studies have demonstrated the ability of thermal feedback to evoke specific emotional responses, investigating dimensions like perceived intensity (cool to hot), valence (unpleasant to pleasant), and arousal (calm to exciting) [12], [13]. However, these studies have primarily focused on limited body sites, such as the palm and wrist, despite recent advancements in thermal feedback devices [14]–[16] that extend coverage to larger areas of the arm, from the dorsum of the hand to the upper arm for immersive and realistic applications. Furthermore, the role of indoor environmental factors, particularly indoor temperature, in shaping thermal feedback perception remains underexplored [17], even though the effects of thermal feedback can depend on these parameters.

To address these gaps, we investigated sensory and emotional responses–perceived intensity, valence, and arousal–by systematically varying the amplitude of change (AoC), rate of change (RoC), and indoor temperature across three body sites on the hand and arm: the dorsum of the hand, forearm, and upper arm. Specifically, we designed 36 thermal feedback patterns using six AoC levels ($\pm 2, 4, 6°C$), two RoC levels ($1, 2°C/s$), and three indoor temperatures ($18, 24, 30°C$). Next, we ran a user study to collect subjective ratings on these patterns and analyzed how the design parameters influenced sensory and emotional ratings. For example, the results revealed that AoC is the primary parameter affecting intensity and arousal ratings across all three body sites, while its influence on valence ratings was observed only for the forearm and upper arm.

In addition to analyzing the impacts of design parameters of thermal feedback, we developed a neural network to predict user ratings and help accelerate the design process. We designed a neural network with two hidden layers and evaluated it on 48 unseen thermal feedback combinations, comparing its performance against three baseline machine learning models. Our model demonstrated state-of-the-art performance, predicting intensity, valence, and arousal ratings with an average RMSE of 5.6736 on a 0–100 scale. This suggests that designers can effectively estimate the effects of thermal feedback on sensations and emotions using our model. Based on our findings, we compile design guidelines for creating thermal feedback patterns to deliver the intended intensity sensations and emotions and discuss future research directions.

II. User Study

A. Hardware Configuration

We designed thermal feedback system using a Peltier module (Multicomp; MCPE-071-10-13; (W) 20.0 × (L) 20.0 × (D) 3.6 mm) for controlled heating and cooling, paired

* Both authors contributed equally to this research.

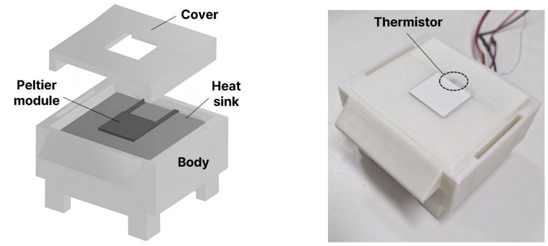

(a) (b)

Fig. 1: Thermal feedback system design: (a) An exploded view of our custom thermal feedback system. (b) A perspective view of our actual system showing the thermistor placement.

with a thermistor (Mouser Electronics; 223Fu3122) to control temperature changes (Figure 1 (a)). In detail, an Arduino UNO regulated the Peltier module's temperature by controlling the motor driver's duty cycle (ShenzenAV; L298n). The cover part contained an aperture ((W) 20.0 × (L) 20.0 mm) to expose the Peltier module, while the contact area ((W) 20.0 × (L) 18.6 mm) was limited by the slop integrated with cover. The thermistor was located between a slop and Peltier module to maintain the target temperature using a PID loop and to prevent the thermistor from measuring participants' skin temperature (Figure 1 (b)). Unlike other designs, this slop provides direct contact between the Peltier module and the participant's skin. A cooling fan affixed under the heat sink was used during rest periods to dissipate residual heat, ensuring consistent initial conditions for each trial. The body part ((W) 77.5 × (L) 68.0 × (D) 42.0 mm) housed all components within its interior and was designed with four pillars to mitigate the transmission of vibrations caused by the cooling fan operation. The cover and body parts were 3D-printed using Poly Lactic Acid (PLA), resulting in a lightweight design for the entire device (85.5 g).

B. Thermal Feedback Design

We created 36 thermal feedback patterns by varying on six amplitude of change (AoC) values ($\pm 2, 4, 6^{\circ}\mathrm{C}$), two rate of change (RoC) values ($1, 2^{\circ}\mathrm{C}/s$), and three indoor temperatures ($18, 24, 30^{\circ}\mathrm{C}$). We selected these three design parameters based on their common use in thermal feedback design (AoC and RoC) [12], [13] and the underexplored influence of indoor environmental factors (i.e., indoor temperatures) [17]. We also considered balancing perception and safety to choose the AoC and RoC values, taking into account the detection thresholds for thermal feedback, which depend on the interaction between AoC and RoC [18], and the pain thresholds of skin temperature [19]. For instance, skin damage can occur if the skin temperature rises above $45^{\circ}\mathrm{C}$ or falls below $18^{\circ}\mathrm{C}$. We ensured that the designed thermal feedback patterns did not produce any pain through a pilot study with three participants. We applied the thermal feedback on three body sites on hand and arm (dorsum of hand, forearm, and upper arm), considering coverage of commercial thermal feedback devices [14]–[16] (Figure 3).

In addition to the 36 thermal feedback patterns used for analyzing the impacts of design parameters and training a predictive model, we created 16 additional patterns to serve as a test set for model evaluation (Section III). In other words, these 16 patterns were excluded from the analysis and model training and were used solely for testing as unseen data. The test set patterns varied on four AoCs ($\pm 3, 5^{\circ}\mathrm{C}$), two RoCs ($0.75, 1.5^{\circ}\mathrm{C}/s$), and two indoor temperatures ($20, 28^{\circ}\mathrm{C}$). As with the training patterns, these were applied to the same three body sites on the hand and arm.

(a)

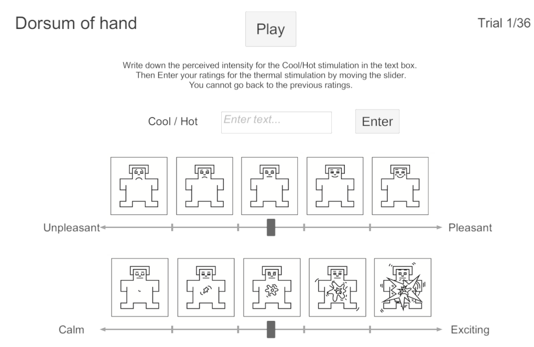

(b)

Fig. 2: A screenshot of the GUI used to collect user responses during the user study: (a) familiarization session and (b) main session.

C. Participants

We recruited 12 participants (six females and six males; 18–31 years old (mean:22.3, SD:1.7)). All participants reported no impairments in thermal perception. Participants completed the user study over five days, with each day's experiment lasting 60 minutes on average (i.e., total duration: around five hours). Participants received $75 USD as compensation.

D. Experiment Procedure

The user study spanned five days to examine the effects of indoor temperature as a design parameter for thermal feedback. We controlled the indoor temperature using a thermostat and verified it with a thermometer. To minimize the influence of humidity on thermal perception [17], we maintained humidity levels around 30% using a humidifier. In other words, each day's experiment was conducted at a specific indoor temperature, with the five indoor temperatures (18, 20, 24, 28, and $30^{\circ}\mathrm{C}$) balanced across the study.

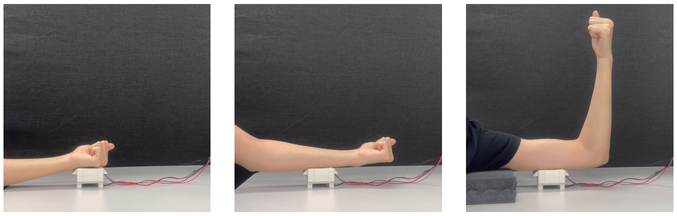

(a) Dorsum of hand (b) Forearm (c) Upper arm

Fig. 3: Three body sites used in the study.

Each day's experiment consisted of three sessions: adaptation, familiarization, and main session. The same structure was followed for all five days. In the adaptation session, after obtaining informed consent, the participants received an introduction for the experiment from the experimenter. Specifically, we instructed the participants to use their right hand to operate the mouse to interact with GUI program while their left hand was secured to the hardware device for consistent data collection (Figure 3). They then adapted to the controlled indoor temperature for 10 minutes to reduce external variability before proceeding to the familiarization session [20]. In the familiarization session, the participants experienced two extreme thermal stimuli (cool/hot) from the stimuli set used in the main session (Figure 2a). They felt these stimuli by clicking buttons in a GUI program. The Peltier device's starting temperature was set to match the typical human skin temperature (31.13°C to 33.77°C), which varied with indoor temperature ranges [21]. Each stimulus lasted 10 seconds, followed by a 30-second break to allow skin temperature to return to its initial resting state [13]. This session familiarized participants with the full range of thermal feedback patterns in a set before they moved on to the main session.

In the main session, participants rated the perceptual intensity, valence, and arousal for all stimuli in the assigned set (Figure 2b). Each day, one of two thermal feedback pattern sets was used under one of five different indoor temperature conditions. Each set contained either 12 patterns (six AoC levels $\times$ two RoC levels; train set) or eight patterns (four AoC levels $\times$ two RoC levels; test set). The order of indoor temperature conditions was randomized across days. Prior research confirmed that thermal perception on one day does not affect perception on subsequent days [17]. The presentation order of body sites was also randomized using a Balanced Latin Square. Although both train and test sets were collected during the user study, only data from the train set were used for analysis (Section II-E). Participants rated perceived intensity using their own scale $(-\infty, \infty)$ by entering a numeric value (negative for cool, positive for hot) into an input field, while rating valence (unpleasant/pleasant) and arousal (calm/exciting) using SAM sliders [22] with 0–100 scale. Participants could play the stimuli multiple times and take breaks as needed.

E. Results

For analysis, we normalized each participant's intensity rating scale to a 0–100 scale using Max-Abs scaling, where values below 50 represent cool sensations and values above 50 represent hot sensations. The standard deviations in intensity, valence, and arousal ratings of the 12 participants for the 36 thermal feedback patterns were 9.90, 15.79, and 17.82 (out of 100), respectively. To examine the effects of the three design parameters (AoC, RoC, and indoor temperature) on intensity, valence, and arousal ratings, we conducted aligned rank transform analysis of variance (ART-ANOVA) tests [23], as the data did not meet the assumptions of normality and homogeneity of variance. The tests were performed for three dimensions (intensity, valence, and arousal ratings) and three hand and arm sites (dorsum of hand, forearm, and upper arm).

TABLE I: Test results for dorsum of hand, forearm, and upper arm, including only significant interaction effects (i.e., no significant differences in AoC$\times$RoC and RoC$\times$Indoor temp.)

Ind. Variable	Dep. Variable	Statistic	η^2
Dorsum of hand			
AoC	Intensity	F(5,385) = 333.8033, p < **0.0001**	0.8126
	Valence	F(5,385) = 1.7488, p = 0.1225	0.0222
	Arousal	F(5,385) = 17.0637, p < **0.0001**	0.1814
RoC	Intensity	F(1,385) = 0.0003, p = 0.9864	< 0.0001
	Valence	F(1,385) = 0.2701, p = 0.6036	0.0007
	Arousal	F(1,385) = 2.0148, p = 0.1566	0.0052
Indoor temperature	Intensity	F(2,385) = 0.0915, p = 0.9126	0.0005
	Valence	F(2,385) = 1.5770, p = 0.2079	0.0081
	Arousal	F(2,385) = 0.4005, p = 0.6703	0.0021
AoC : Indoor temperature	Valence	F(10,385) = 4.3060, p < **0.0001**	0.1006
Forearm			
AoC	Intensity	F(5,385) = 433.3081, p < **0.0001**	0.8491
	Valence	F(5,385) = 6.1340, p < **0.0001**	0.0738
	Arousal	F(5,385) = 12.9227, p < **0.0001**	0.1437
RoC	Intensity	F(1,385) = 2.5498, p = 0.1111	0.0066
	Valence	F(1,385) = 0.1629, p = 0.6867	0.0004
	Arousal	F(1,385) = 0.0399, p = 0.8418	0.0001
Indoor temperature	Intensity	F(2,385) = 1.6008, p = 0.2031	0.0082
	Valence	F(2,385) = 2.9754, p = 0.0522	0.0152
	Arousal	F(2,385) = 0.5856, p = 0.5573	0.0030
AoC : Indoor temperature	Valence	F(10,385) = 4.7386, p < **0.0001**	0.1096
Upper arm			
AoC	Intensity	F(5,385) = 542.5301, p < **0.0001**	0.8757
	Valence	F(5,385) = 3.2621, p = **0.0067**	0.0406
	Arousal	F(5,385) = 21.1343, p < **0.0001**	0.2154
RoC	Intensity	F(1,385) = 0.0349, p = 0.8519	< 0.0001
	Valence	F(1,385) = 0.1421, p = 0.7065	0.0004
	Arousal	F(1,385) = 0.0277, p = 0.8680	< 0.0001
Indoor temperature	Intensity	F(2,385) = 2.6363, p = 0.0729	0.0135
	Valence	F(2,385) = 2.0907, p = 0.1250	0.0107
	Arousal	F(2,385) = 7.1080, p = **0.0009**	0.0356
AoC : Indoor temperature	Valence	F(10,385) = 7.9920, p < **0.0001**	0.1719
	Arousal	F(10,385) = 2.1187, p = **0.0223**	0.0522

The test results showed that AoC is the primary parameter affecting intensity sensations and emotions across the three body sites, except for the effects of indoor temperature on arousal on the upper arm (Table I). AoC significantly impacted intensity and arousal ratings across all body sites, while influencing valence ratings for the forearm and upper arm. However, despite the statistical significance, the effect sizes for AoC on valence were all below 0.1, suggesting limited practical impact [24], [25]. Post-hoc pairwise comparisons using ART-C [26] with Bonferroni corrections showed significant differences in AoCs for all possible pattern combinations for intensity, 20–30% combinations for valence, and 60% combinations for arousal. Significant differences in valence existed for the interactions between AoC and indoor temperature across all three body sites. However, for arousal, the interaction was significant only for the upper arm, although the practical impact was minimal ($\eta^2 < 0.1$).

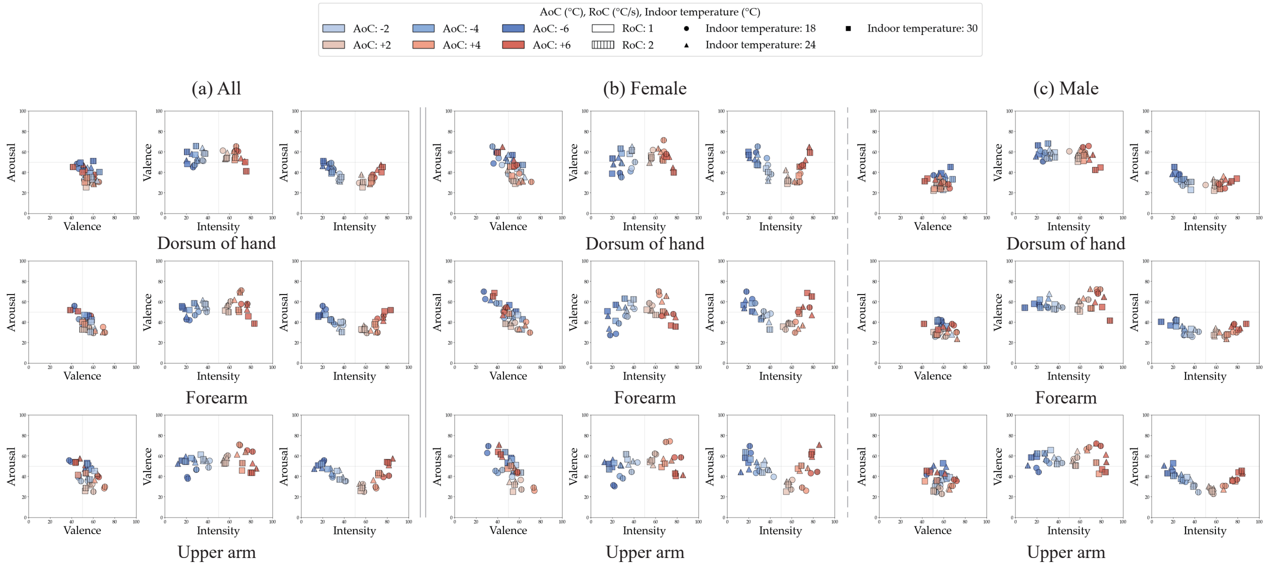

Fig. 4: Plots showing intensity, valence, and arousal ratings for each body site under varying AoC, RoC, and indoor temperature conditions. Data was visualized for (a) all participants, (b) female participants, and (c) male participants.

The data collected from all participants showed that most valence and arousal ratings fell within the range of 20 to 80, suggesting that the thermal feedback patterns used in the user study did not elicit extreme emotional responses (Figure 4 (a)). Correlations between valence and arousal ratings varied across body sites, with values of -0.51, -0.69, and -0.52, all with $p < 0.01$, for the dorsum of the hand, forearm, and upper arm, respectively (Figure 4 (a), left). The intensity and valence ratings exhibited weak correlations but showed roughly symmetric distributions across the three body sites: dorsum of the hand ($r = 0.08$), forearm ($r = 0.24$), and upper arm ($r = 0.23$), all significant at $p < 0.01$ (Figure 4 (a), middle). For the forearm and upper arm, increasing indoor temperature led to a shift in the relationship between intensity and valence: as intensity increased, valence transitioned from an increasing to a decreasing trend. For example, at an indoor temperature of 18°C, cooler sensations evoked more unpleasant emotions, while hotter sensations evoked more pleasant emotions. Conversely, at an indoor temperature of 30°C, cooler sensations evoked more pleasant emotions, while hotter sensations evoked more unpleasant emotions. As a result, the combined distributions formed a horizontal hourglass-shaped pattern, which was more distinct for the forearm and upper arm compared to the dorsum of the hand. The intensity and arousal ratings showed 'V'-shaped patterns across body sites (Figure 4 (a), right).

The data divided by gender revealed differences in ratings between females and males (Figure 4 (b) and (c)). Females exhibited higher mean valence and arousal ratings (57.85 for valence, 46.79 for arousal) than males (51.62 for valence, 33.45 for arousal) for the 36 identical thermal feedback patterns, while mean intensity ratings remained similar between the two groups. Standard deviations were higher for females across all three dimensions, with differences of 1.62, 1.72, and 3.31 for intensity, valence, and arousal ratings, respectively. Notably, females reported a wider range of valence ratings (20 to 80) compared to males (40 to 80). Similarly, female arousal ratings typically ranged between 20 and 70, a broader range than the male arousal ratings of 20 to 50. As a result, male emotional ratings were primarily located in the 4th quadrant of the valence-arousal plots across body sites. Correlations in ratings between genders were 0.97 (intensity), 0.43 (valence), and 0.61 (arousal), all with $p < 0.01$.

III. Prediction Model for Thermal Feedback

Using the collected sensory and emotional ratings of 36 thermal feedback patterns across three body sites, we developed a model to predict these ratings using five inputs: AoC, RoC, indoor temperature, body site, and gender. Since body site and gender were categorical variables, we applied ordinal encoding to convert them into numerical values (ordinal variables): dorsum of the hand = 0, forearm = 1, and upper arm = 2; female = 0 and male = 1.

A. Network Architecture

Despite the relatively small dataset, we employed a deep neural network (DNN) for prediction, as the rating trends exhibit non-linearity (Figure 4). The network consisted of two hidden layers with 128 and 64 nodes (Figure 5). Each layer used the ReLU activation function and included batch normalization [29] and dropout [30] layers to improve generalization

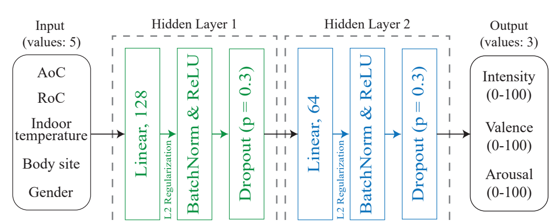

Fig. 5: Network architecture of the proposed DNN model.

TABLE II: Comparison of RMSE values for intensity, valence, and arousal predictions across baseline models.

Method	Network	Intensity	Valence	Arousal	Average RMSE
Baseline	Linear Regression	4.8949	8.0944	7.7304	6.9065
	Support Vector Regression Machine [27]	11.3912	7.9337	9.8112	9.7120
	Random Forest [28]	7.2560	9.7557	8.7852	8.5990
Proposed Method	Deep Neural Network	4.3772	6.2478	6.3957	5.6736

and prevent overfitting. The dropout rate was set to 0.3 for both layers. The final layer outputted three values corresponding to intensity, valence, and arousal ratings, each on a scale of 0–100.

B. Implementation

We implemented the DNN using PyTorch [31] and trained it on an NVIDIA RTX 2080 Ti GPU. The model was optimized with Adam (weight decay = 1e-5) using MSE loss, a batch size of 32, and a learning rate of 0.001 for 1000 epochs. Five-fold cross-validation was applied to ensure robust and reliable performance.

C. Evaluation

We evaluated the performance of our model against three baseline machine learning models using 48 unseen thermal feedback combinations (four AoC levels $\times$ two RoC levels $\times$ two indoor temperatures $\times$ three body sites). The baseline models included Linear Regression, Support Vector Regression Machine [27], and Random Forest [28]. All baseline models were trained on the same thermal feedback patterns as our model.

D. Results

Our DNN model outperformed the three baselines across intensity, valence, and arousal ratings, achieving the lowest averaged RMSE (5.6736) (Table II). While Linear Regression performed reasonably well on the test set (RMSE = 6.9065), it failed to capture the nonlinearity in the data effectively (Figure 6 (a)). In contrast, our model successfully captured the nonlinearity, producing horizontal hourglass-shaped predictions for intensity-valence ratings and 'V'-shaped predictions for intensity-arousal ratings (Figure 6 (b)).

IV. Discussion

Based on our study and model evaluation results, we present four design guidelines for creating thermal feedback patterns and discuss implications for future research and applications.

A. Design Guidelines

1. The amplitude of change (AoC) is the most effective design parameter, especially for the forearm and upper arm. AoC significantly influenced perceived intensity and arousal across all three body sites (Table I). These findings suggest that the AoC values ($\pm 2, 4, 6°C$) used in the study were sufficient to effectively impact these ratings, given the discrimination thresholds for AoC (0.025–1.3°C for cooling and 0.01–3.3°C for warming [32]–[34]). In addition, AoC modulated valence on the forearm and upper arm, though with small effect sizes, making these sites ideal for generating a wide range of user experiences. We conjecture that the lower just noticeable difference (JND) at the forearm and upper arm, compared to the JND at the hand [12], [34], along with differences in activation patterns between the hand and arm in response to emotional experiences [35], may explain the observed body site effects. Future work should investigate the effects of body sites on valence in greater depth.

2. The rate of change (RoC) over $1°\mathrm{C}/s$ is not an effective parameter for human sensations and emotions. Our analysis did not reveal significant impacts of RoCs (1 and $2°\mathrm{C}/s$) on sensations or emotions across the three body sites, based on both statistical results and visualizations. Given that only RoC values slower than $0.1°\mathrm{C}/s$ influenced the thermal perception threshold [36], the RoC values used in our study may be too fast to affect intensity and emotional ratings. However, employing RoC values slower than $0.1°\mathrm{C}/s$ may not be practical for real-world applications that require rapidly conveying information to users via thermal displays. Therefore, designers can fix the RoC values over $1°\mathrm{C}/s$ according to the technical capabilities of their thermal feedback devices and instead focus on adjusting other parameters to enhance the user experience.

3. Designers should create thermal feedback patterns while considering that the effects of AoC on emotions can depend on indoor temperature. Interaction between AoC and indoor temperature had significant impact on valence across three body sites on the hand and arm (Table I). Moreover, we also observed that the positive relationship between valence and intensity at 18°C diminished as the indoor temperature increased to 24°C, eventually turning negative at 30°C (Figure 4 (a), middle). This effect was more pronounced on the forearm and upper arm compared to the dorsum of the hand. These findings suggest that while indoor temperature may not need to be a major consideration when designing feedback for the hand, designers should carefully account for its effects on emotion for the arm.

4. Consider gender differences in thermal feedback effects on valence and arousal. Although gender is known not to influence thermal thresholds [37], the thermal feedback patterns used in our study formed distinct distributions in emotional space between females and males (Figure 4 (b) and (c)). These results suggest that psychological gender differences play a role, aligning with findings reported in [38]. Similar to the literature, our study showed that males exhibited greater thermal comfort than females (valence: 51.62 (F) vs. 57.85 (M)), while females tended to express greater dissatisfaction with the thermal feedback (valence range: 20–80 (F) vs. 40–80 (M)). Additionally, males reported lower mean arousal ratings (arousal: 46.79 (F) vs. 33.45 (M)), possibly due to their stronger thermal regulation ability in transient environments [38]. These differences led to moderate to strong correlations in emotions between genders (valence: $r = 0.43$,

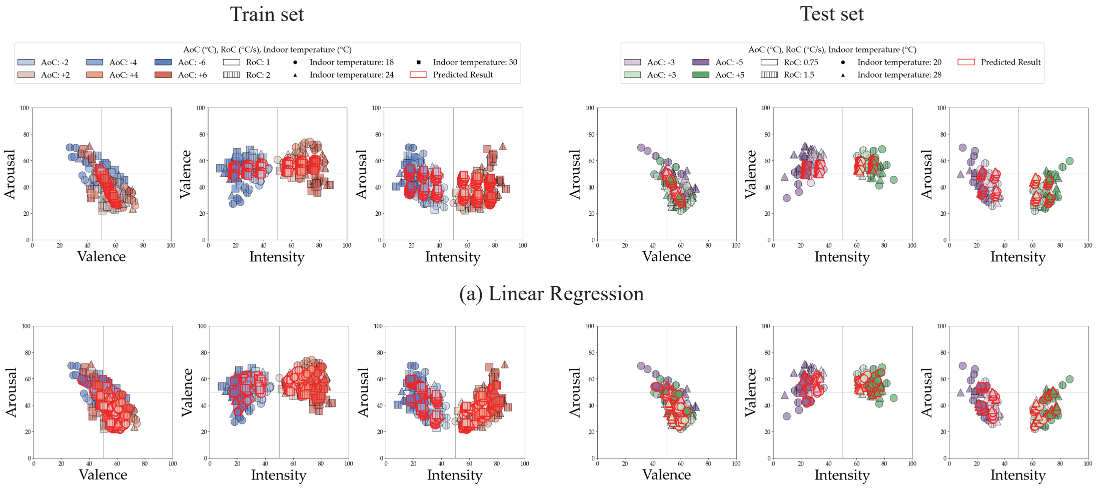

(a) Linear Regression

(b) Our model (DNN)

Fig. 6: Prediction results of (a) Linear Regression and (b) our model on the training and test datasets. Our model successfully captures the nonlinear trends in the data.

arousal: $r = 0.61$) compared to a very strong correlation in intensity sensation ($r = 0.97$). Thus, designers should consider both physiological and psychological gender effects when creating thermal feedback patterns to provide personalized user experiences.

B. Implications for Future Work

We outline how our systematic investigations and prediction model can inform future research and influence haptic design practices.

Designers can use our guidelines and the proposed model to estimate intensity sensations and emotions when prototyping new thermal feedback patterns. Investigating sensory and emotional responses to new thermal feedback patterns can be time-consuming for designers. Our guidelines provide insights into the efficacy of design parameters–AoC, RoC, indoor temperature, and gender–across three body sites on the hand and arm, based on statistical analysis and visualizations. Additionally, our model demonstrated a low RMSE (5.6736) when predicting sensory and emotional ratings (on a 0–100 scale) for unseen thermal feedback patterns. This allows designers to quickly estimate the sensations and emotions elicited at specific body sites by inputting five values: AoC, RoC, indoor temperature, body sites, and gender. Future work could expand the model by incorporating additional design parameters, such as the area of stimulation [18], and extending its application to other body sites, enabling rapid prototyping across a broader range of thermal feedback designs.

Our model can inform the development of future computational models to predict sensations and emotions conveyed by diverse haptic stimuli. Recent research has proposed computational models to predict various subjective attributes of haptic stimuli, such as the perceptual dissimilarity of vibrotactile icons (i.e., Tactons) [39] and tactile attributes of textured surfaces [40]. Our work contributes to this field by enabling the prediction of thermal perception based on five input values of AoC, RoC, indoor temperature, body site, and gender. Future research can extend our approach beyond static conditions to incorporate dynamic contexts, considering the influence of proprioception on thermal perception. In addition, with the growing integration of thermal feedback into both traditional haptic technologies, such as force feedback and mechanical vibrations, and emerging technologies, such as electrovibrations [41] and mid-air ultrasound vibrations [42], future work could focus on developing computational models for multimodal feedback. Examples include mechanical vibration-thermal feedback [43] and mid-air vibration-thermal feedback [44], which have the potential to create more immersive and dynamic haptic experiences.

V. Conclusion

Thermal feedback presents new opportunities for conveying sensations and emotions across diverse applications and scenarios. In this work, we designed thermal feedback patterns and conducted a user study, resulting in design guidelines and a deep neural network model capable of accurately predicting user sensations and emotions. We hope that our guidelines and model will enable designers to craft rich and engaging user experiences, fostering creativity and driving advancements in the application of thermal feedback within haptic design.

Acknowledgment

This work was supported by research grants from VILLUM FONDEN (VIL50296, 25%), the National Science Foundation (#2339707, 25%), the MSIT (Ministry of Science, ICT), Korea, under the Global Research Support Program in the Digital Field program (RS-2024-00419561, 25%) supervised by the IITP (Institute for Information & Communications Technology Planning & Evaluation), and the Culture, Sports and Tourism R&D Program through the Korea Creative Content Agency funded by the Ministry of Culture, Sports and Tourism in 2023 (RS-2023-00226263, 25%).

REFERENCES

[1] S. Günther, F. Müller, D. Schön, O. Elmoghazy, M. Mühlhäuser, and M. Schmitz, "Therminator: Understanding the interdependency of visual and on-body thermal feedback in virtual reality," in *Proceedings of the 2020 CHI Conference on Human Factors in Computing Systems*, 2020, pp. 1–14.

[2] R. L. Peiris, W. Peng, Z. Chen, L. Chan, and K. Minamizawa, "Thermovr: Exploring integrated thermal haptic feedback with head mounted displays," in *Proceedings of the 2017 CHI Conference on Human Factors in Computing Systems*, 2017, pp. 5452–5456.

[3] S. Cai, P. Ke, T. Narumi, and K. Zhu, "Thermairglove: A pneumatic glove for thermal perception and material identification in virtual reality," in *2020 IEEE conference on virtual reality and 3D user interfaces (VR)*. IEEE, 2020, pp. 248–257.

[4] A. Nasser and K. Hasan, "Thermograsp: Enabling localized thermal feedback on fingers for precision grasps in virtual reality," *Proceedings of the ACM on Human-Computer Interaction*, vol. 8, no. MHCI, pp. 1–21, 2024.

[5] V. Kotsev, A. Nikolev, K. Pawlak, and M. Löchtefeld, "Investigating the usage of thermal feedback as an active game element," in *Proceedings of the 16th International Conference on Mobile and Ubiquitous Multimedia*, 2017, pp. 91–95.

[6] M. Löchtefeld, T. Lappalainen, J. Väyrynen, A. Colley, and J. Häkkilä, "Comparing thermal and haptic feedback mechanisms for game controllers," in *Proceedings of the 2017 CHI Conference Extended Abstracts on Human Factors in Computing Systems*, 2017, pp. 1829–1836.

[7] M. Guiatni, V. Riboulet, C. Duriez, A. Kheddar, and S. Cotin, "A combined force and thermal feedback interface for minimally invasive procedures simulation," *Ieee/Asme Transactions On Mechatronics*, vol. 18, no. 3, pp. 1170–1181, 2012.

[8] X. Meng, J. Han, G. Chernyshov, K. Ragozin, and K. Kunze, "Thermaldrive-towards situation awareness over thermal feedback in automated driving scenarios," in *Companion Proceedings of the 27th International Conference on Intelligent User Interfaces*, 2022, pp. 101–104.

[9] S. T. Fiske, A. J. Cuddy, and P. Glick, "Universal dimensions of social cognition: Warmth and competence," *Trends in cognitive sciences*, vol. 11, no. 2, pp. 77–83, 2007.

[10] L. E. Williams and J. A. Bargh, "Experiencing physical warmth promotes interpersonal warmth," *Science*, vol. 322, no. 5901, pp. 606–607, 2008.

[11] H. IJzerman and G. R. Semin, "The thermometer of social relations: Mapping social proximity on temperature," *Psychological science*, vol. 20, no. 10, pp. 1214–1220, 2009.

[12] G. Wilson, M. Halvey, S. A. Brewster, and S. A. Hughes, "Some like it hot: thermal feedback for mobile devices," in *Proceedings of the SIGCHI Conference on Human Factors in Computing Systems*, 2011, pp. 2555–2564.

[13] G. Wilson, D. Dobrev, and S. A. Brewster, "Hot under the collar: mapping thermal feedback to dimensional models of emotion," in *proceedings of the 2016 CHI conference on human factors in computing systems*, 2016, pp. 4838–4849.

[14] WEART, "Touchdiver haptic glove," https://weart.it/, accessed: 2025-01-21.

[15] TEGWAY, "Thermoreal: Temperature feedback haptic device," http://tegway.co/tegway/, 2025, accessed: 2025-01-21.

[16] Teslasuit, "Teslasuit: Full body haptic feedback, motion capture, and biometric sensing suit," https://teslasuit.io/, accessed: 2025-01-21.

[17] M. Halvey, G. Wilson, S. Brewster, and S. Hughes, """ baby it's cold outside" the influence of ambient temperature and humidity on thermal feedback," in *Proceedings of the SIGCHI Conference on Human Factors in Computing Systems*, 2012, pp. 715–724.

[18] L. A. Jones and M. Berris, "The psychophysics of temperature perception and thermal-interface design," in *Proceedings 10th symposium on haptic interfaces for virtual environment and teleoperator systems. HAPTICS 2002*. IEEE, 2002, pp. 137–142.

[19] I. Darian-Smith and K. O. Johnson, "Thermal sensibility and thermoreceptors," *Journal of Investigative Dermatology*, vol. 69, no. 1, pp. 146–153, 1977.

[20] A. R. Ismail, N. Jusoh, N. K. Makhtar, N. K. Khamis, R. M. Zein, and N. H. C. Hassan, "Cfd study on thermal implication towards human body in office environment," *Journal of Advanced Research in Fluid Mechanics and Thermal Sciences*, vol. 85, no. 1, pp. 125–134, 2021.

[21] I. A. Strigo, F. Carli, and M. C. Bushnell, "Effect of ambient temperature on human pain and temperature perception." *Anesthesiology*, vol. 92, no. 3, pp. 699–707, 2000.

[22] A. Betella and P. F. Verschure, "The affective slider: A digital self-assessment scale for the measurement of human emotions," *PloS one*, vol. 11, no. 2, p. e0148037, 2016.

[23] J. O. Wobbrock, L. Findlater, D. Gergle, and J. J. Higgins, "The aligned rank transform for nonparametric factorial analyses using only anova procedures," in *Proceedings of the SIGCHI conference on human factors in computing systems*, 2011, pp. 143–146.

[24] R. J. Calin-Jageman and G. Cumming, "The new statistics for better science: Ask how much, how uncertain, and what else is known," *The American Statistician*, vol. 73, no. sup1, pp. 271–280, 2019.

[25] R. Nuzzo, "Statistical errors: P values, the'gold standard'of statistical validity, are not as reliable as many scientists assume," *Nature*, vol. 506, no. 7487, pp. 150–153, 2014.

[26] L. A. Elkin, M. Kay, J. J. Higgins, and J. O. Wobbrock, "An aligned rank transform procedure for multifactor contrast tests," in *The 34th annual ACM symposium on user interface software and technology*, 2021, pp. 754–768.

[27] H. Drucker, C. J. Burges, L. Kaufman, A. Smola, and V. Vapnik, "Support vector regression machines," *Advances in neural information processing systems*, vol. 9, 1996.

[28] L. Breiman, "Random forests," *Machine learning*, vol. 45, pp. 5–32, 2001.

[29] S. Ioffe, "Batch normalization: Accelerating deep network training by reducing internal covariate shift," *arXiv preprint arXiv:1502.03167*, 2015.

[30] N. Srivastava, G. Hinton, A. Krizhevsky, I. Sutskever, and R. Salakhutdinov, "Dropout: a simple way to prevent neural networks from overfitting," *The journal of machine learning research*, vol. 15, no. 1, pp. 1929–1958, 2014.

[31] Pytorch, "Pytorch: An open source deep learning framework," https://pytorch.org/, accessed: 2025-01-21.

[32] K. O. Johnson, I. Darian-Smith, and C. LaMotte, "Peripheral neural determinants of temperature discrimination in man: a correlative study of responses to cooling skin." *Journal of Neurophysiology*, vol. 36, no. 2, pp. 347–370, 1973.

[33] A. M. L. Kappers and M. A. Plaisier, "Thermal perception and thermal devices used on body parts other than hand or face," *IEEE transactions on haptics*, vol. 12, no. 4, pp. 386–399, 2019.

[34] V. H. Lilliesköld and E. Nordh, "Method-of-limits; cold and warm perception thresholds at proximal and distal body regions," *Clinical neurophysiology practice*, vol. 3, pp. 134–140, 2018.

[35] L. Nummenmaa, E. Glerean, R. Hari, and J. K. Hietanen, "Bodily maps of emotions," *Proceedings of the National Academy of Sciences*, vol. 111, no. 2, pp. 646–651, 2014.

[36] D. R. Kenshalo, C. E. Holmes, and P. B. Wood, "Warm and cool thresholds as a function of rate of stimulus temperature change," *Perception & Psychophysics*, vol. 3, no. 2, pp. 81–84, 1968.

[37] L. Gray, J. C. Stevens, and L. E. Marks, "Thermal stimulus thresholds: Sources of variability," *Physiology & Behavior*, vol. 29, no. 2, pp. 355–360, 1982.

[38] X. Xu, H. Zhang, G. Wu, Z. Lian, and H. Xu, "Sex differences in body temperature and thermal perception under stable and transient thermal environments: A comparative study," *Science of The Total Environment*, vol. 951, p. 175323, 2024.

[39] C. Lim and G. Park, "Can a computer tell differences between vibrations?: Physiology-based computational model for perceptual dissimilarity prediction," in *Proceedings of the 2023 CHI Conference on Human Factors in Computing Systems*, 2023, pp. 1–15.

[40] M. I. Awan, W. Hassan, and S. Jeon, "Predicting perceptual haptic attributes of textured surface from tactile data based on deep cnn-lstm network," in *Proceedings of the 29th ACM Symposium on Virtual Reality Software and Technology*, 2023, pp. 1–9.

[41] O. Bau, I. Poupyrev, A. Israr, and C. Harrison, "Teslatouch: electrovibration for touch surfaces," in *Proceedings of the 23nd annual ACM symposium on User interface software and technology*, 2010, pp. 283–292.

[42] C. Lim, G. Park, and H. Seifi, "Designing distinguishable mid-air ultrasound tactons with temporal parameters," in *Proceedings of the CHI Conference on Human Factors in Computing Systems*, 2024, pp. 1–18.

[43] H. Wang, Y. Singhal, H. Gil, and J. R. Kim, "Thermal masking: When the illusion takes over the real," in *Proceedings of the CHI Conference on Human Factors in Computing Systems*, 2024, pp. 1–16.
[44] H. Wang, Y. Singhal, and J. R. Kim, "Let it snow: Designing snowfall experience in vr," *Proceedings of the ACM on Interactive, Mobile, Wearable and Ubiquitous Technologies*, vol. 8, no. 2, pp. 1–24, 2024.